

Spatial Distribution of a Midblock-Associating Homopolymer Blended into a Triblock Copolymer

Suck-Hyun Lee[†] and J. T. Koberstein*

Institute of Material Science and Department of Chemical Engineering, University of Connecticut, Storrs, Connecticut 06269-3136

X. Quan

AT&T Bell Laboratories, Murray Hill, New Jersey 07974

I. Gancarz

Technical University of Wroclaw, Wroclaw, Poland

G. D. Wignall

NCSASR, Oak Ridge National Laboratory, Oak Ridge, Tennessee 37830

F. C. Wilson

E. I. Du Pont de Nemours, Inc., Wilmington, Delaware 19880

*Received October 12, 1993; Revised Manuscript Received March 1, 1994**

ABSTRACT: The spatial distribution of a midblock associating homopolymer confined within the lamellar microdomain structure of a triblock copolymer is probed with small angle neutron scattering experiments. The materials examined are poly(styrene-*b*-[saturated 1,2-butadiene]-*b*-styrene) triblock copolymers to which a low molecular weight poly(saturated 1,2-butadiene) homopolymer has been added. The butadienes are saturated with either hydrogen, deuterium, or mixtures of the two gases in order to vary their neutron scattering contrast with respect to polystyrene. The results of contrast matching experiments demonstrate that there is a strong tendency for the homopolymer to localize at the center of the midblock microdomain. Experimental scattering profiles are modeled using one-dimensional scattering density profiles in order to obtain a quantitative description of the blend morphologies. This modeling indicates that two distinct scenarios exist for homopolymer localization in a triblock copolymer: one wherein the microdomain structure contracts and a second wherein there is an expansion of the microdomain. Possible origins of this behavior are proposed on the basis of the consideration of the configurations available to the midblock sequence, that is, tie chains that traverse the midblock domain, or loops that enter and exit the midblock microdomain through the same interface.

Introduction

Block copolymer blends with homopolymers present complex morphologies and mechanical properties as a result of the nature of their molecular structure and interactions. Composite mechanical theories often fail in properly describing the mechanical properties of these complex microcomposites. Blends of poly(2,6-dimethyl-1,3-phenylene oxide) with poly(styrene-*b*-butadiene-*b*-styrene) copolymers have been studied¹ because the addition of the homopolymer can raise the glass transition temperature and softening point of the hard block, thereby extending the temperature range where these important thermoplastic elastomers are applicable. A single mixed hard phase was observed for the blends, indicating that the homopolymer dissolved within the hard phase, but the dynamic mechanical properties of the blends showed significant departures from the predictions of various composite models.

In our own laboratories, we have studied the morphology and mechanical properties of elastomeric hydrogenated poly(1,2-butadiene)s blended into a poly(styrene-*b*-hydrogenated 1,2-butadiene-*b*-styrene) copolymer (S-hB-S).²⁻⁵ The plateau modulus of such blends, based upon considerations of composite theory, is expected to decrease

upon blending of additional rubbery homopolymer. Contrary to expectation, we observed the moduli to be equal to or even greater than that of the neat block copolymer. The addition of homopolymers to block copolymers clearly can produce synergistic effects on mechanical properties that cannot be explained solely by consideration of the macroscopic material structures. It is likely that synergism of this nature in block copolymer blends is related to the unusual chain configurations imposed upon the molecular segments due to the constraints of the block copolymer microdomain structure.

The morphology of a neat S-hB-S triblock copolymer, established through previous characterization²⁻⁵ is pictured schematically in Figure 1a. The polystyrene end blocks segregate from the rubbery midblock to form a lamellar microdomain structure. The midblock chains within this structure must adopt extended conformations³ (i.e., depicted by the shaded ovals in the figure) in order to fill space at the center of the lamellar microdomain. Upon addition of low molecular weight hB homopolymer, the average lamellar repeat period was found to decrease, perhaps due to relaxation of the space filling requirements of the midblock sequence as a result of the presence of the homopolymer. Initially, we proposed^{2,3} that this would most likely occur if the homopolymer were preferentially distributed at the center of the midblock microdomain, as depicted in the lamellar contraction-localization model (Figure 1b). That is, the lamellar thickness can decrease

* To whom correspondence should be addressed.

[†] Present address: Department of Applied Chemistry, Ajou University, 5 Woncheondong, Suwan, South Korea 440-749.

* Abstract published in *Advance ACS Abstracts*, May 1, 1994.

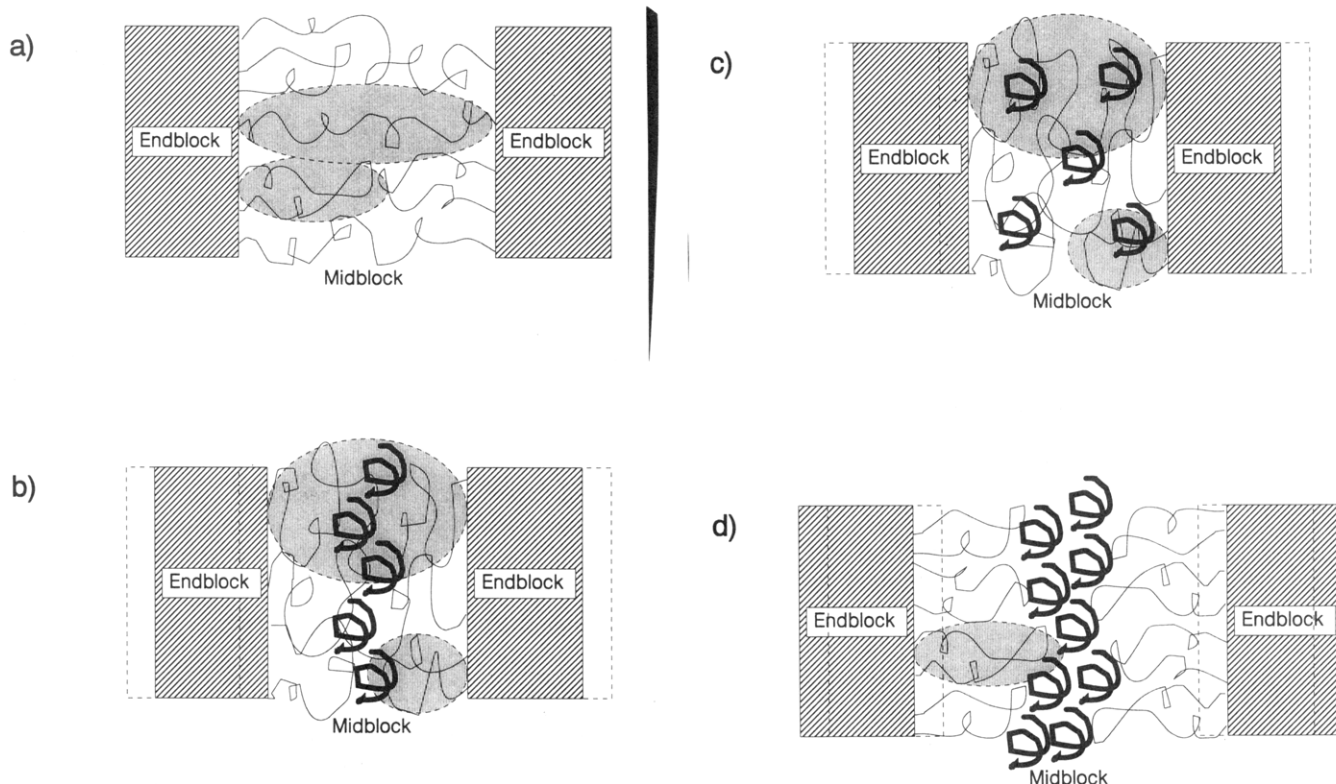


Figure 1. Models for homopolymer distribution within the midblock microdomain of a triblock copolymer. (a) Neat triblock copolymer. Chains are stretched (as indicated by the shaded ellipses) in order to fill space at the center of the microdomain. (b) Microdomain contraction-localization model. The microdomain contracts as homopolymer localizes in order to reduce the extension of the midblock sequences. (c) Microdomain contraction-uniform distribution model. The microdomains are contracted, but the homopolymer is uniformly distributed. (d) Microdomain expansion-double layer model. In regions where there are primarily loop configurations, the midblock sequences retain the configurations of the neat triblock. Homopolymer chains localize at the microdomain center, splitting the microdomains into two midblock double layers.

upon homopolymer addition if, in the process, the midblock sequences are allowed to relax into less extended conformations (i.e., indicated by the decreased aspect ratios for the shaded ovals in Figure 1b). Since that time, homopolymer localization of this nature has been observed in studies on diblock copolymer/homopolymer blends,⁶⁻⁸ and a theoretical basis for this behavior has been presented.⁹

The molecular environment of the midblock sequence of a triblock copolymer differs markedly from that of end block sequences, and also from those of a diblock copolymer, since both ends of the sequence are connected to another block. While these conformational differences do not appreciably affect the microdomain dimensions of block copolymers, they drastically change the mechanical properties of the materials, to the extent that virtually all commercially important block copolymers have triblock architecture. Other important distinctions between diblock and triblock copolymers arise when their blends with midblock associating homopolymers are considered. The homopolymer solubility of a triblock, for example, is limited by how much the midblock "tie chains" chain can be stretched. Furthermore, the existence of tie chains traversing the midblock microdomain opposes the segregation of homopolymer to the center of the microdomain, especially for homopolymer molecular weights approaching those of the midblock sequence. The scenario pictured in Figure 1c, where the homopolymer is uniformly distributed, is therefore a possibility that must also be considered.

These conformational limitations are relaxed, to a certain extent, by the number of midblock chains that form looped configurations, that is, leave and enter from the same microdomain boundary rather than traverse

across the entire midblock microdomain (e.g., see Figure 1a). In the extreme case where only loops are present, one can also envisage a morphology (i.e., microdomain expansion-double layer model) as depicted in Figure 1d, where the homopolymer simply divides the bilayer looped structure, resulting in microdomain expansion. Double layer morphologies of this nature have already been observed when preferential solvent was added to a crystallizable block copolymer.¹⁰

It is clear that a deeper understanding of the properties of triblock copolymer blends requires a more detailed characterization of their structure on a molecular level. Toward this end, we report herein the results of a SANS investigation regarding the spatial distribution of a midblock-associating homopolymer confined within the lamellar microdomains of a triblock copolymer. In particular, we examine which if any of the morphological models previously proposed for diblock copolymers blends may be appropriate for these triblock copolymer blends.

Experimental Section

In order to separate the various structural contributions of block copolymer/homopolymer blends, it is necessary to synthesize a series of homopolymers and block copolymers with identical chain architectures, but with controllable neutron scattering length densities (i.e., contrast). For this purpose we have selected a material system based upon styrene and butadiene monomers. The first step in preparing the triblock copolymer is the synthesis of a poly(styrene-*b*-1,2-butadiene-*b*-styrene) precursor by anionic methods. For the homopolymer, a similar precursor, poly(1,2-butadiene), is prepared. The neutron contrast is then controlled by selectively saturating the polybutadiene segments of the precursors with either hydrogen, deuterium, or mixtures of the two gases. In this fashion, it is possible to match

Table 1. Characterization Results for the Butadiene Precursor and Saturated Polymers

designation	description	M_n	M_w/M_n	% PS (w/w)	% 1,2-PB addition
S-B-S	triblock precursor		1.15	49	91
S-hB-S	hydrogen saturated triblock	112K	1.32	49	91
S-pmB-S	phase-matched saturated triblock	117K	1.28	49	91
PB	butadiene precursor		1.05	0	95
PhB	hydrogen saturated analog	11K	1.14	0	95
PpmB	phase-matched saturated analog	10K	1.09	0	95

Table 2. Neutron Contrast Densities of Saturated Analogs Relative to Polystyrene

homopolymer	contrast density difference (cm^{-1}) $\times 10^{12}$
hydrogen saturated butadiene	-2.85
deuterium saturated butadiene (2 deuterium per mer)	0.35
phase-matched saturated butadiene (1.8 deuterium per mer)	≈ 0.03

Table 3. Description of Blends

designation	block copolymer	homopolymer	% homopolymer (w/w)
blend A	S-hB-S	PhB	20
blend B	S-pmB-S	PhB	20
blend C	S-hB-S	PpmB	20

the contrast of the resultant hydrogenated polybutadiene to that of polystyrene, thus enabling separation of scattering functions by contrast matching techniques. A ratio of 1:9 hydrogen to deuterium was employed to produce the phase-matched materials. The procedures employed for homopolymer and block copolymer synthesis and for the selective saturation of the polybutadiene segments have been reported previously.²⁻⁵

Molecular characterization results²⁻⁵ for the materials employed are presented in Table 1. Three triblocks are made, all symmetric with essentially identical sequence lengths (30–60–30K MW), but differing in contrast according to the gas used for hydrogenation. The contrasts with respect to polystyrene are given in Table 2. The hydrogen saturated analog has a much lower contrast than polystyrene, the deuterium saturated analog has a contrast slightly higher than polystyrene, and the so-called "phase-matched" (i.e., containing 1.8 deuterium per mer) analog has no contrast with respect to polystyrene. The absence of contrast for the phase-matched triblock has been previously demonstrated.³ The homopolymers (ca. MW 10K) are also essentially identical except for their contrast (see Tables 1 and 2). The microstructures of the butadiene precursors are primarily the 1,2-product, such that the hydrogenated products can be considered equivalent to atactic poly(1-butene) and would be noncrystalline.

Blends of the three triblocks, all containing 20% by weight of the appropriate homopolymer, were prepared by solvent casting from dichloromethane, followed by vacuum annealing at 140 °C for several hours. Transmission electron microscopy shows that the morphology of the blends is predominantly lamellar. Homopolymer macrodomains were not observed, indicating that the homopolymer was incorporated almost exclusively within the midblock microdomains.^{9,12} Three blends were prepared from the various contrast labeled materials, as described in Table 3. These various contrast combinations allow for the determination of the homopolymer distribution.

SANS data were collected at the National Center for Small Angle Scattering Research at Oak Ridge National Laboratory, using sample-to-detector distances ranging from 3 to 18 m, as described previously.²⁻⁴ These data have been calibrated against known standards to obtain absolute intensity values and have been corrected for incoherent scattering. Small angle X-ray scattering (SAXS) data were collected with a high resolution Bonse-Hart camera and with a Kratky slit camera. The former data were smoothed and desmeared using the method of Schmidt and Hight,¹¹ while the latter data are employed directly without calibration.

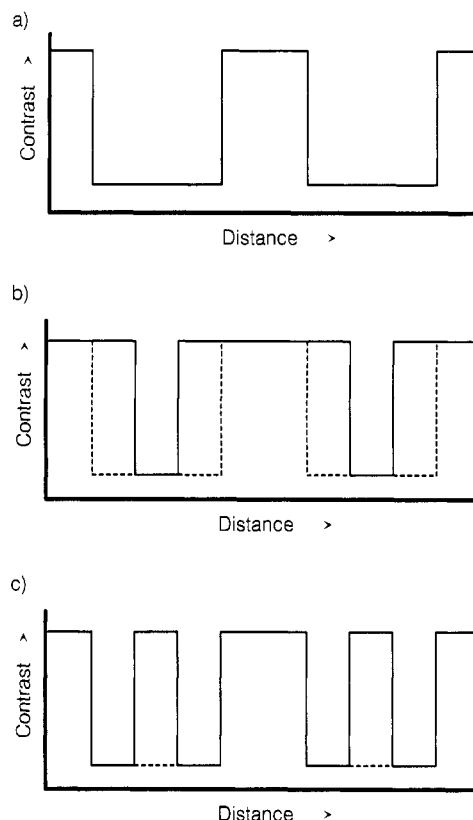


Figure 2. Linear contrast density models assuming complete partitioning of the homopolymer at the center of the midblock microdomain: (a) blend A; (b) blend B; (c) blend C.

Results and Discussion

SAXS experiments were performed on the three blend systems in order to ensure that there were no significant effects of the deuterium labeling or solvent casting on the basic blend morphologies. Deuterium labeling does not affect the X-ray scattering contrast, and therefore the three blends should give essentially identical SAXS profiles. The basic features of the SAXS patterns for the three blends were found to be equivalent,² demonstrating that their overall morphologies are essentially the same.

In contrast to the SAXS profiles, the SANS curves for the three blends reflect directly the distribution of homopolymer within the microdomain. If the homopolymer is distributed homogeneously throughout the midblock microdomain, the contrasts will be different for the three systems, but the contrast normalized density profiles (i.e., the dashed profiles in Figure 2) and shapes of the scattering profiles will be identical. If however the homopolymer localizes preferentially at the center of the midblock microdomain, as depicted in Figure 1b, the contrast density profiles for the three blends will differ markedly. For blend C for example, the localized homopolymer has the same contrast as that of the styrene end block and, in the extreme case of complete segregation, would yield the contrast density profile shown schematically in Figure 2c. The structure factor, or normalized neutron scattering intensity, for the three blends is related

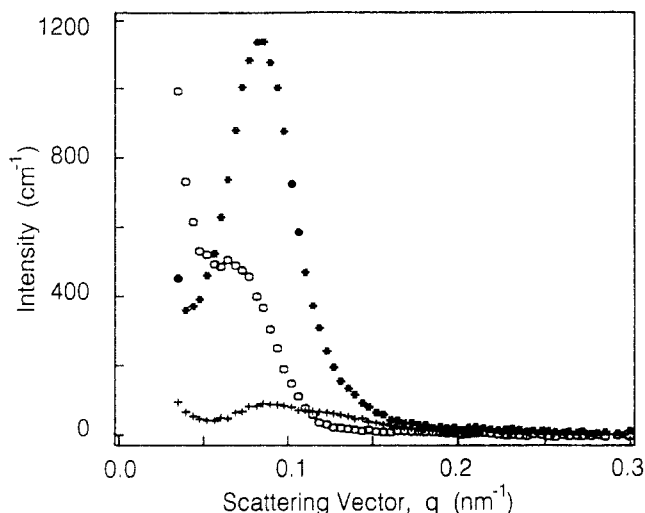


Figure 3. SANS profiles for blends containing 20% by wt homopolymer: blend A (asterisks), blend B (open squares), blend C (plusses).

to this density profile and will thus reflect directly the homopolymer distribution. If the distribution is homogeneous, the three normalized SANS profiles will superimpose; if the homopolymer distribution within the midblock microdomain is not homogeneous, the three scattering profiles will be different.

The SANS profiles for the three blends, shown in Figure 3, differ markedly from one another, indicating that the homopolymer is not homogeneously distributed throughout the midblock microdomain. Blend A contains fully protonated butadiene in both the homopolymer and block copolymer. The scattering profile for this blend will be essentially independent of the homopolymer distribution, neglecting any effects of the density difference between the homopolymer and poly(1-butene) copolymer sequence. The profile will always look like that of Figure 2a and reflect the overall dimensions of the microdomains.

Blend B contains the phase matched block copolymer and fully protonated homopolymer. Its scattering profile reflects only the distribution of the homopolymer and will always look somewhat like the profile shown in Figure 2b. If the homopolymer is confined to reside within the midblock microdomain and is distributed homogeneously throughout this microdomain, the structure factor would be identical to that of blend A, and the scattering profiles would have the same shape. The shape of the blend B curve differs from that of the A blend, indicating an inhomogeneous distribution of homopolymer. The scattering maximum is more poorly defined for the B blend, showing that the homopolymer distribution is more disordered than the distribution of the midblock microdomains. This observation is consistent with what has been seen and predicted previously for diblock blends.^{8,9} That is, there is a broad distribution function of homopolymer within the microdomain, with the maximum homopolymer density occurring at the center and falling off toward the microdomain boundaries.

An inhomogeneous distribution of homopolymer is clearly indicated in the scattering profile for blend C. Here, localization of the homopolymer leads to the creation of a new correlation length that is about half of the interlamellar distance (see Figure 1c). This localization is signaled by the appearance of a secondary scattering maximum (Figure 3) at approximately twice the scattering vector of the primary maximum observed for blend A.

The simple comparisons of scattering peak positions and shapes presented above are only qualitative in nature

and can be misleading for complicated systems. A more quantitative understanding of the homopolymer distribution requires the application of a more detailed analysis of the scattering profiles. The approach we employ for this purpose is based upon the construction of linear density models and has been discussed thoroughly in a previous paper.⁵ Similar approaches have been frequently applied to investigate the structures of other lamellar systems,¹² and only the basic principles will be presented here. The starting point of the analysis is to construct a linear density model for the distribution of contrast perpendicular to the lamellae. These models represent the fluctuation in contrast, $\eta(z)$, from the material average contrast as a function of the distance z , and are analogous to the contrast profiles sketched in Figure 2. After a model density profile is constructed manually, the correlation function is calculated by self-convolution of this profile

$$\gamma_{1D}(z) = \int_0^\infty \eta(\xi - z)\eta(\xi) d\xi \quad (1)$$

The integration is performed numerically from the constructed density profiles. In the real structure, the spatial coherence of the microdomains is not infinite, but is limited by the grain size and other types of disorder. The correlation function will be damped out by the occurrence of this disorder. We have previously been successful in representing the disorder in the system by applying a Lorentzian damping function, $P(z)$ with a single disorder parameter, σ

$$P(z) = \frac{1}{1 + (z/\sigma)^2} \quad (2)$$

With this damping function, the effective correlation function becomes

$$\gamma_{1D,e}(z) = \gamma_{1D}(z)P(z) \quad (3)$$

The one-dimensional intensity for the model contrast density profile can then be calculated by a simple numerical one-dimensional Fourier transform

$$I_{1D}(s) = K \int_0^\infty \gamma_{1D,e}(z) \cos(qz) dz \quad (4)$$

The model intensity calculated in this fashion can then be compared to the experimental one-dimensional intensity. For samples that are globally isotropic, as in the present case, the experimental one-dimensional intensity is obtained by simply multiplying the experimental intensity by the correction factor $4\pi q^2$.

The neutron scattering lengths are normalized using the following relation

$$b_i = a_i - \nu_i \frac{a_0}{\nu_0} \quad (5)$$

where a_i and ν_i are the scattering length and specific volume of the i th mer, respectively, and the subscript zero denotes those values averaged over the whole material. These values are further normalized to lie in the range -1 to $+1$ by setting a_0 equal to zero. This normalization is not important to our analysis since we are primarily interested in the spatial correlation and not the overall contrast. We also include a diffuse interphase in our model density profiles (i.e., a linear interphase gradient of width 5 nm is employed in the model profiles); however the width of the interphase does not significantly affect the correlation functions.⁹

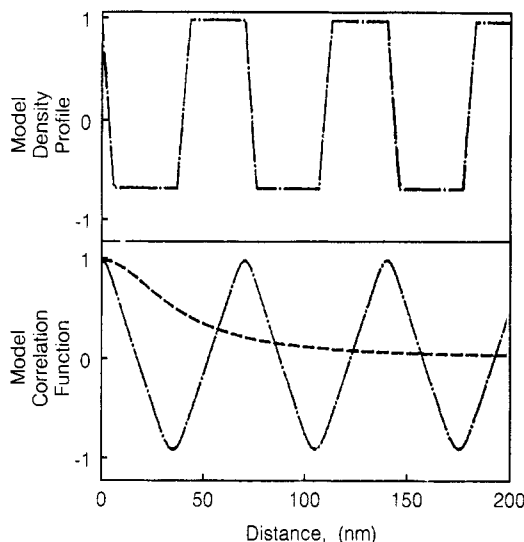


Figure 4. Linear density profile model (top) and model correlation function (bottom) for blend A. The dashed line in the lower part of the figure denotes the Lorentzian function used to damp the correlation function.

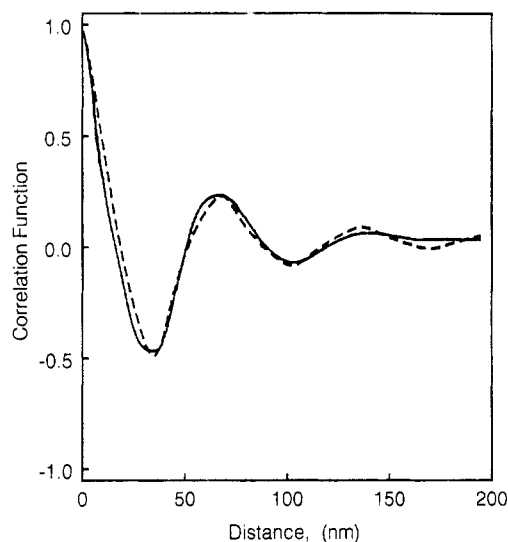


Figure 5. Comparison of the experimental (solid line) and model (dashed line) correlation functions for blend A.

The modeling is first applied to blend A, which has a density profile similar to that shown in Figure 2a. There are three parameters involved in the fit: the two microdomain dimensions and the Lorentzian damping function. In reality, only one microdomain dimension need be adjusted, since the total repeat distance is easily determined from the position of the first maximum in the correlation function.⁵ The Lorentzian damping parameter is also readily obtained from the manner in which the correlation function damps out. The best model is obtained as the minimum error between the experimental and the model generated correlation functions. The results of this modeling applied to blend A are shown in Figures 4 and 5. The high density regions of the model density profile represent polystyrene, while the low density region is the mixed microdomain containing PhB homopolymer and the PhB midblock sequence. Excellent agreement is obtained between the experimental and model correlation functions, demonstrating that the simple lamellar model with one disorder parameter provides a reasonable representation of the scattering behavior. From these results, we determine that the one-dimensional lamellar repeat distance is 68 nm, including polystyrene lamellae of average thickness 27 nm and a midblock microdomain, containing

both homopolymer and midblock hydrogenated polybutadiene chains, with an average thickness of 31 nm. The half-width of the Lorentzian damping function is estimated to be 36 nm. These values describe the overall lamellar microdomain morphology and will be used in the analysis of the other blends, since the SAXS data showed their morphologies to be equivalent.

The same modeling procedure applied to the data for blend B produces the following parameters: 70 nm for the repeat distance, 27 nm for the end block microdomain thickness, and 33 nm for the midblock microdomain thickness. These numbers are effectively equal to those found for blend A; however, the Lorentzian damping function is broader for blend B (i.e., $\sigma = 30$ nm). Even with the broader damping function, the experimental correlation function is found to be broader than the model correlation function. This observation indicates that the distribution of homopolymer is broader than that represented by the simple trapezoidal density profile (e.g., similar to that of Figure 4) used in the analysis. Further modeling to obtain the precise distribution of homopolymer was not attempted.

The scattering profile for blend C is the most sensitive to inhomogeneities in the homopolymer distribution, since they lead to the creation of a new correlation length, as shown schematically in Figure 2c. Indeed, two correlation lengths are apparent in Figure 3, qualitatively consistent with the expectations of the microdomain contraction-localization model pictured in Figure 1b. The validity of this model can be tested quantitatively by the model correlation function analysis. To construct the required linear density model, we employ the two overall microdomain dimensions that have already been measured for blend A and assume that the disorder parameter is identical. The dimension of the segregated homopolymer region is obtained from the known composition of the blend; that is, the homopolymer constitutes one-third of the mass of the mixed midblock microdomain, and its dimension is thus one-third that of the midblock (i.e., assuming equal density for all PhB species). Diffuse phase boundary thicknesses of the segregated homopolymer region were assumed to be equal to those at the microdomain interface. There are therefore no adjustable parameters employed in this comparison.

The linear density profile constructed in this manner and a comparison between the associated model and experimental one-dimensional scattering intensities for blend C are shown in Figure 6. The model produces a weak maximum at about $\log q = -2.0$, corresponding to the 68-nm distance between polystyrene lamellae, a primary maximum at 34 nm ($\log q \approx -1.7$) corresponding to the homopolymer-end block distance, and a third maximum at 25 nm ($\log q \approx -1.6$), associated with the distance between the two minima in the density profile of the midblock microdomain. Although the experimental curve does show evidence of small maxima or shoulders at these three positions, the model intensity does not reproduce the dominant feature in the experimental intensity profile, a maximum observed at about -1.85 (44 nm) on the $\log q$ axis. The relative intensities of the maxima in the scattering profile are sensitive to the end block thickness, while their positions change only slightly with thickness. The central maximum increases with an increase in the midblock thickness, while the outer maxima increase with the end block thickness, as can be seen from the two model scattering profiles shown in Figure 6b. Whereas the qualitative comparison of scattering profiles supported a model wherein the homopolymer is localized

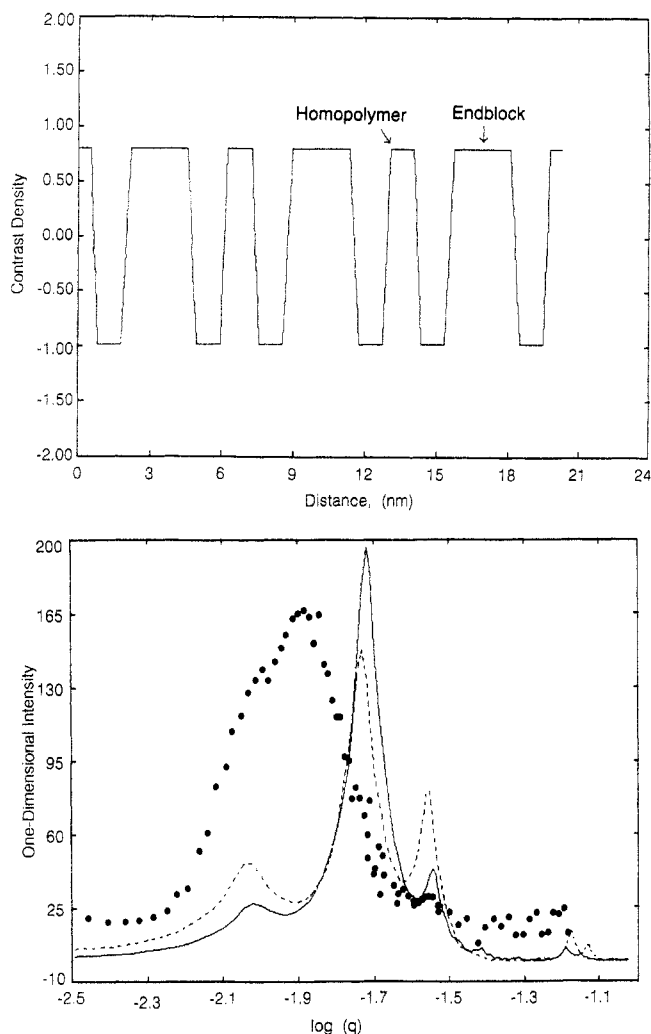


Figure 6. Microdomain contraction-localization model (Figure 1b) in which the homopolymer localizes preferentially at the center of the midblock microdomain: (a, top) linear density profile; (b, bottom) experimental (points) and model (lines) scattering profiles. The solid line denotes the results for a polystyrene end block microdomain thickness of 26 nm, and the dashed line is the result for a thickness of 28 nm.

at the center of the midblock microdomain, a quantitative comparison demonstrates that this model reproduces only the secondary features of the experimental scattering curve for blend C.

The distribution of homopolymer within a midblock microdomain is therefore more complicated than the idealistic model presented in Figure 1b. Specifically, this model provides no explanation for the primary maximum, with 44-nm period, found in the experimental scattering curve. In searching for a better explanation, we will confine ourselves to models that have already been proposed in the literature, and for which we can generate model density profiles without any adjustable parameters.

The possibility that the homopolymer was homogeneously distributed, as depicted in the microdomain contraction-uniform distribution model (see Figure 1c), was therefore examined. It is reasonable that this structure might occur in regions of the material where the midblock chains primarily traverse the midblock and thus cannot deplete themselves from the center of the microdomain. In applying this model, we have allowed for two homopolymer depletion zones that are required at the microdomain interfaces (see Figure 7a). Otherwise, the profile is similar to that used for blend A (see Figure 4). The microdomain dimensions and disorder parameter are taken from the results for blend A, and the contrast of the

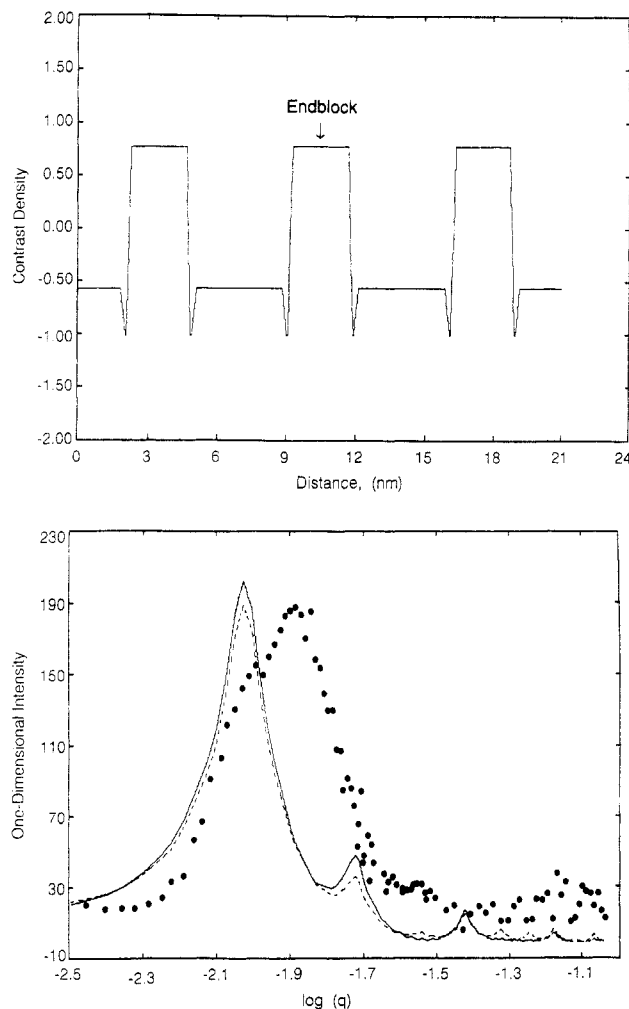


Figure 7. Microdomain contraction-uniform distribution model (Figure 1c) in which the homopolymer is homogeneously distributed throughout the midblock microdomain: (a, top) linear density profile; (b, bottom) experimental (points) and model (lines) scattering profiles. The solid line denotes the results for a polystyrene end block microdomain thickness of 26 nm, and the dashed line is the result for a thickness of 28 nm.

mixed midblock microdomain is calculated from the known composition and contrasts of the PhB and PpmB moieties. Again, there are no adjustable parameters employed in this comparison. The model produces two primary maxima at 68 and 34 nm (i.e., $\log q$ of about -2.0 and -1.7 , respectively) but again does not reproduce the primary experimental maximum observed at 44 nm ($\log q \approx -1.85$).

From the results for these two models, it is clear that alteration of the distribution of the homopolymer within a contracted lamellar structure cannot account for the most prominent maximum in the scattering peak and that there must exist within the blend another distinct morphology. The only other model that has been shown previously to exist in block copolymer blends is the microdomain expansion-double layer model presented in Figure 1d. At first, it is not obvious how this model, developed to explain the swelling behavior of crystalline block copolymers, might be appropriate to triblock copolymer/homopolymer blends, but its plausibility becomes apparent when one considers the possibility of looped configurations of the midblock sequence. There are basically only two configurations available to the midblock sequences: they may traverse the entire midblock microdomain, entering on one lamellar interface and exiting on the other, or they may enter and exit the lamella from the same interface. Both possibilities are expected, and there will naturally be spatial fluctuations in the

concentration of each conformation, especially if one considers that these structures actually form in solution during solvent casting. Solvent casting with a preferential solvent for the midblock, for example, would be expected to promote correlated regions of looped configurations, as shown in the model. In such regions, the homopolymer is expected to behave in a manner similar to that of the double layer concept: it will simply push the two double layers apart.

A model of this nature can be again constructed without any adjustable parameters. The polystyrene microdomain thickness (ca. 28 nm) and midblock half-domain thicknesses (ca. 21 nm, i.e., half of 42 nm) were determined from modeling on the neat triblock.⁵ The thickness of the homopolymer region splitting the two bilayers can be obtained from the known composition and should be essentially equal to that of the half-domain thickness, or 21 nm. This model then predicts a homopolymer-end block center-to-center distance given by half of the polystyrene and homopolymer thicknesses plus the half-domain thickness, for a total periodicity of about 45.5 nm. This compares well to the experimental primary maximum observed at about 44 nm. In the actual modeling, we have adjusted the homopolymer thickness in the profile to a value of 18 nm, in order to match the experimental maximum (see Figure 8a). The other parameters have been fixed as described above. The adjustment corresponds to about a 10% reduction in the homopolymer content assumed to lie between the bilayers and does not qualitatively change the features in the scattering profile. The model profile for this microdomain expansion-double layer model and the associated one-dimensional scattering profile are shown in Figure 8. The model reproduces the primary maxima, but not the various shoulders observed in the experimental scattering profile. Changes in the distribution of the homopolymer, denoted by the dashed profile in Figure 8a, also do not appreciably change the scattering function (see Figure 8b).

It appears that at least two or three models are required to reproduce all of the features observed in the experimental scattering profile for blend C. If there are regions of heterogeneity in structure due to localized differences in the midblock chain conformation (i.e., loops and tie chains), it is reasonable to expect behavior of this nature. If these regions are independent of one another the scattering profile will simply reflect the weighted contribution of each model.

A reasonable representation of the scattering intensity for blend C can indeed be constructed by adding contributions from the three models discussed herein, as shown in Figure 9a. To generate the model curve, we assumed that two one-fourth portions of the structure correspond to each of the two microdomain contraction models and that the remaining half of the structure corresponds to the expanded bilayer model. It should be reemphasized that there are no adjustable parameters used in these models; all of the parameters have been estimated from available data and measurements on blend A. Both the positions of the scattering maxima and their relative intensities are properly accounted for with these three relatively simple yet reasonable models.

As a check on the consistency of the modeling approach, we have also taken the SANS models employed for blend C and used them to predict the SAXS profile measured for blend C. The model reproduces well the experimental SAXS curve, as shown in Figure 9b, confirming that the composite scattering curve constructed from the three model density profiles is a reasonable description of the

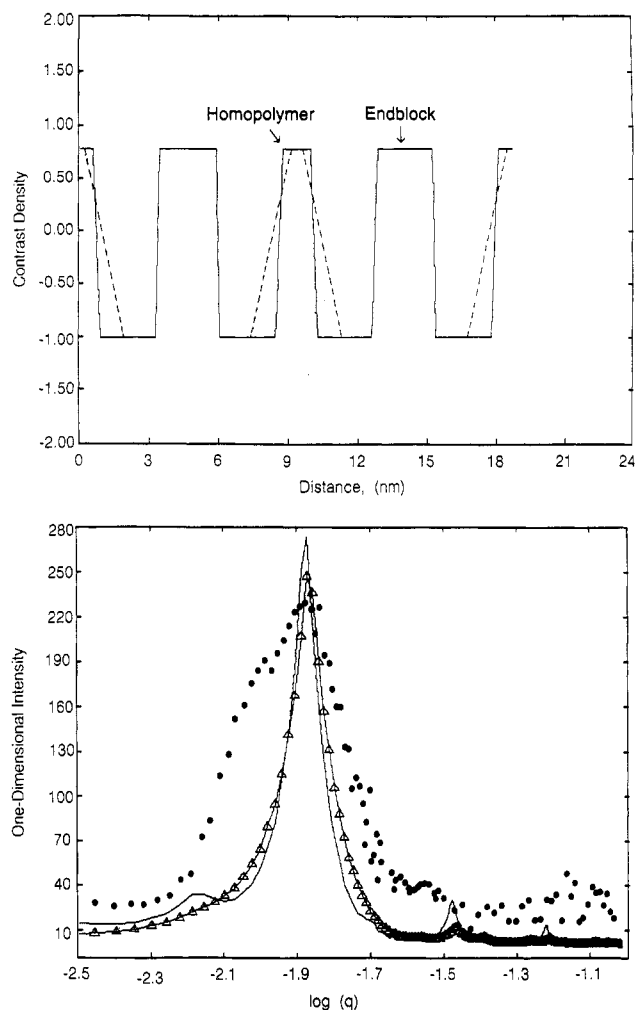


Figure 8. Microdomain expansion-double layer model (Figure 1d) in which the homopolymer localizes preferentially at the center of the midblock microdomain, residing between two copolymer midblock layers. (a, top) Linear density profiles. The solid line shows a sharp distribution of homopolymer at the center of the microdomain, and the dashed line shows a broad distribution. (b, bottom) Experimental (points) and model (lines) scattering profiles. The solid line denotes the results for the broad distribution profile, and the line marked with triangles denotes the scattering profile corresponding to the broad distribution density profile.

structure of the blend. These three models represent extreme cases. They are not meant to provide an exact description of the homopolymer distribution, but rather to produce a reasonable explanation for the observed periodicities in the SANS profiles. For example, the two models involving domain contraction, one with localization and one without, could be equivalently represented with a single model employing a broader distribution of homopolymer. This is reasonable considering that both models account for about one-fourth of the structure of the material and produce similar repeat periods. The results indicate that the environment of the midblock in these blends is heterogeneous: about half of the material appears to correspond to expanded structures, perhaps occurring where there are primarily looped configurations, while the other half consists of contracted structures where there is a broad distribution of homopolymer centered at the middle of the midblock microdomain.

Summary Discussion

The results of these neutron scattering experiments demonstrate that the distribution of a low molecular weight midblock-associating homopolymer dissolved within a

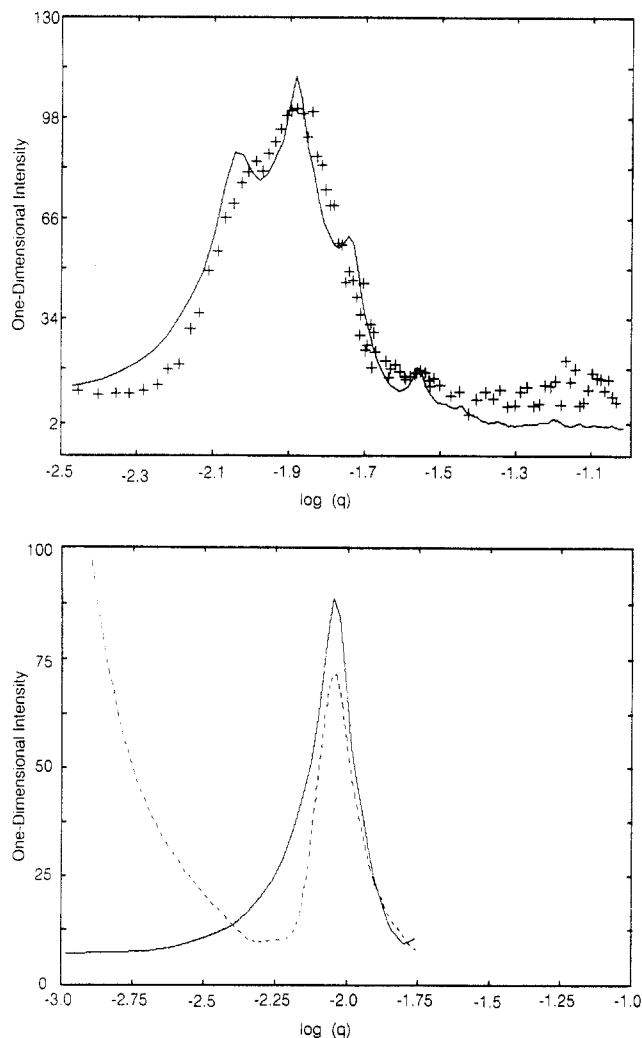


Figure 9. Comparison of the experimental one-dimensional scattering patterns with a model profile generated by assuming that half of the structure is given by the microdomain expansion-double layer model and that the other half of the structure is equally divided between the microdomain contraction-localization and microdomain contraction-uniform distribution models: (a, top) SANS, experimental (pluses) and model (solid line); (b, bottom) SAXS, experimental Bonse-Hart results (dashed line) and model (solid line).

triblock copolymer is inhomogeneous. Through the use of contrast variation techniques we have shown that there is a strong tendency for the homopolymer to localize preferentially at the center of the midblock microdomain. In order to explain the scattering curves it is necessary to invoke two scenarios for this localization: one wherein the microdomain structure contracts and another wherein the microdomain structure expands. We propose two basic driving forces that would lead to this behavior. The first involves the release of constraints on the normally extended midblock sequences. The localization of homopolymer at the center of the lamellar microdomains can ease these conformational constraints, thereby accounting for the contraction in the average lamellar thickness observed by

SAXS⁵ upon homopolymer addition. The second explanation for homopolymer localization with microdomain expansion arises from consideration of the possible conformations available to the midblock sequences. The midblock sequence may either traverse directly through a lamellae, entering on one side and exiting on the other or manifest a looped configuration entering and leaving from the same lamellar interface. In regions where looped configurations dominate, the homopolymer may simply localize between two layers (i.e., bilayers), leading to an expansion of the lamellae in this region.

The data therefore demonstrate that there is a rather heterogeneous structure inherent to the midblock microdomain of these blends, where there is lamellar expansion, perhaps in regions where there are primarily looped configurations, and lamellar contraction, perhaps in regions rich in traversing tie chains. This behavior is distinct from that of diblock copolymer blends, due to the additional constraints imposed on the copolymer and homopolymer configurations in the midblock microdomain, and may provide a molecular basis for understanding the unusual synergistic mechanical properties observed for blends of triblock copolymers and midblock-associating homopolymers.

Acknowledgment. The authors wish to acknowledge financial support provided by the Cottrell Research Program of the Research Corp., and the Petroleum Research Fund, administered by the American Chemical Society. The work at ORNL was sponsored in part by the NSF Grant No. DMR-7724459 through Interagency Agreement No. 40-636-77 with the U.S. Department of Energy under Contract No. DE-AC05-84OR21400 to Martin Marietta Energy Systems, Inc. Partial support was also provided through grants from The Shell Development Co. and the University of Connecticut Research Foundation. A portion of this work was performed while some of the authors (X.Q., I.G., and J.T.K.) were associated with Princeton University.

References and Notes

- (1) Tucker, P. S.; Barlow, J. W.; Paul, D. R. *Macromolecules* **1988**, *21*, 1678.
- (2) Quan, X. Ph.D. Dissertation, Princeton University, 1986.
- (3) Quan, X.; Gancarz, I.; Koberstein, J. T.; Wignall, G. D. *J. Polym. Sci., Polym. Phys. Ed.* **1987**, *25*, 641.
- (4) Quan, X.; Gancarz, I.; Koberstein, J. T.; Wignall, G. D. *Macromolecules* **1987**, *20*, 1432.
- (5) Baetzold, J. P.; Gancarz, I.; Quan, X.; Koberstein, J. T. *Macromolecules*, submitted for publication.
- (6) Hashimoto, T.; Tanaka, H.; Hasegawa, H. *Macromolecules* **1990**, *23*, 4378.
- (7) Berney, C. V.; Cheng, P. L.; Cohen, R. *Macromolecules* **1988**, *21*, 2235.
- (8) Mayes, A. M.; Russell, T. P.; Satija, S. K.; Kajkrzak, C. F. *Macromolecules* **1992**, *25*, 6523.
- (9) Shull, K. R.; Winey, K. I. *Macromolecules* **1992**, *25*, 2637.
- (10) (a) Gervais, M.; Gallot, B. *Makromol. Chem.* **1977**, *178*, 1577. (b) Gervais, M.; Gallot, B. *Makromol. Chem.* **1973**, *174*, 193.
- (11) Schmidt, P. W.; Hight, R. *Acta Crystallogr.* **1960**, *13*, 480.
- (12) For a general reference see: Feigin, L. A.; Svergun, D. I. *Structure Analysis by Small Angle X-Ray and Neutron Scattering*; Taylor, G. W., Ed.; Plenum Press: New York, 1987.